International Journal of Applied Earth Observations and Geoinformation 97 (2021) 102293

Contents lists available at ScienceDirect

International Journal of Applied Earth Observations and Geoinformation

journal homepage: www.elsevier.com/locate/jag

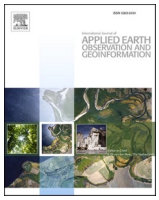

Mapping mangrove dynamics and colonization patterns at the Suriname coast using historic satellite data and the LandTrendr algorithm

Steven M. de Jong [a,*], Youchen Shen [a,b], Job de Vries [a], Ginny Bijnaar [a,c], Barend van Maanen [d], Pieter Augustinus [a], Pita Verweij [a]

[a] Faculty of Geosciences, Utrecht University, the Netherlands
[b] Division of Environmental Epidemiology, Institute for Risk Assessment Sciences, Utrecht University, the Netherlands
[c] Anton de Kom University, Paramaribo, Suriname
[d] College of Life and Environmental Sciences, University of Exeter, UK

ARTICLE INFO

Keywords:
Mangrove colonization
Mangrove patterns
Historic satellite data
Google Earth Engine
LandTrendr
Suriname

ABSTRACT

Mangroves play an important role in protecting coasts against wave energy and storms. Mangrove ecosystems provide important habitats for fauna and flora and are an important carbon sink. Loss of mangroves forest may lead to enhanced coastal erosion. Mangroves are complex ecosystems and processes of settling and development are not fully understood. Characterizing the rates and patterns of mangrove gains and losses is needed to better understand the functioning of mangrove ecosystems, how mangrove dynamics are linked to coastal morphological behaviour and how human interference with the coastal system impacts mangroves. Here we present a study of the mangrove ecosystems at the Suriname coast, which are relatively pristine and characterized by strong dynamics due to migrating mudbanks along the coast. Satellite images between 2000 and 2018, available in the historic satellite image archives, were analysed using the LandTrendr (Landsat-based detection of trends in disturbance and recovery) algorithm to identify locations of mangrove erosion, mangrove colonization, surface areas of change and patterns of settlement, as indicated by (sudden) changes in NDVI. The algorithm requires careful setting of various parameters for successful detection of (abrupt) temporal changes in mangrove coverage. The algorithm was evaluated on its robustness using various parameter settings. Results show the value of the timeseries of Landsat imagery to detect locations of coastal erosion of up to 50 m/yr and accretion where loss or settlement of mangroves is prevailing between 2000 and 2018. Locally differences are very large. An overall westward mangrove progression along the coast is apparent from the images and probably linked to mud bank migration. Various patterns of mangrove colonization and development such as arc-, zonal- and patch-arrangements were identified, although at some locations the Landsat resolution of 30 m is somewhat coarse to allow detailed analysis. The success and robustness of the LandTrendr algorithm are controlled by NDVI threshold values, number of allowed breakpoints in the timeseries and fitting parameters. The presented method requires further testing and evaluation but is a promising tool for semi-automatic detection of coastal mangrove erosion and colonization that can be applied to other mangrove ecosystems in the world. The satellite timeseries analyses generate valuable information on coastal dynamics, which is helpful to identify coastal areas prone to erosion and mangrove retreat and provide as such a valuable tool for coastal management and protection.

1. Introduction

Mangrove ecosystems play a key role in protecting low-lying coasts against storms, waves and sea-level rise (Toorman et al., 2018; Van Bijsterveldt et al. 2020). Mangroves create habitats for fish, birds, benthos and are an efficient carbon sink (Barbier et al., 2011; Saintilan et al., 2020; Spalding et al., 2010). In the second half of the 20th century, about one-third of mangroves were lost worldwide (Alongi, 2002). Building with Nature projects stimulating the resettlement and development of mangroves are ongoing at various locations in the world to restore coastal protection along vulnerable coasts and require knowledge on these complex ecosystems (Winterwerp et al., 2013, 2016; Yang et al., 2008; Lewis, 2005). Mangroves thrive in brackish water of intertidal areas in (sub)tropical regions (Spalding et al., 2010).

* Corresponding author.
E-mail address: s.m.dejong@uu.nl (S.M. de Jong).

https://doi.org/10.1016/j.jag.2020.102293
Received 13 November 2020; Received in revised form 23 December 2020; Accepted 23 December 2020

Environmental factors affecting colonization processes such as floating mangrove seedlings and the spatial development of mangrove forests are not yet fully understood, as these are the result from the interaction between both local and regional processes with various feedbacks (Balke et al., 2013). For example, a delicate balance between currents, sediment fluxes, wave and wind conditions, and tidal elevation is required for young mangrove plants to root and grow, the so-called *windows of opportunities* (Hu et al., 2015; Balke et al., 2014). Mangroves have been observed to settle in distinct zonal or arc-shaped patterns (Fromard et al., 2004); understanding where and why these patterns occur is important ecosystem knowledge. At the same time, so-called bio-morphodynamic models are being developed to investigate the processes and conditions under which mangrove forests can develop sustainably and how human actions interfere (Liu et al., 2003; Winterwerp et al., 2013; Xie et al., 2020; Van Maanen et al., 2015). Research into human impact on mangroves in relation to environmental factors is so far limited (Richards & Friess, 2016; Hamilton & Friess, 2018). Bio-morphodynamic models are therefore useful to develop generic scenarios of coastal evolution and mangrove responses under, for example, changing mud supply and habitat availability, and compare these with current conditions to make mangrove restoration a success. The predictive quality of these models depends on our knowledge of the driving processes of erosion and progradation of mangrove coasts. Such information can be gathered from remote sensing images enabling mangrove change monitoring over various scales of space and time and in diverse environmental settings.

Recent developments in satellite remote sensing provide new means of studying long-term dynamics at the earth surface over large areas (Helder et al., 2018; Liu et al., 2018; van Deijns et al., 2020; Zhua et al., 2019). Examples are the Historic Satellite Data Archive comprising free of charge NASA-Landsat and ESA Sentinel images (Zhua et al., 2019) in Google Earth Engine (Gorelick et al., 2017), and ESA-DIAS initiatives (Copernicus, 2020). Such datasets are also extremely useful for analysis of areas with frequent cloud cover in the (sub)tropics, due to their high temporal image availability (NASA-EO, 2020). Here, we use the Landsat satellite image archive to study mangroves at the Suriname coast in north-eastern South America. Available satellite imagery allows to effectively investigate mangrove behaviour over larger spatial and temporal scales with sufficient temporal resolution. The algorithm LandTrendr: 'Landsat-based detection of trends in disturbance and recovery' (Kennedy and Braaten, 2020) is used for quasi-automated change detection in the time series of Landsat satellite imagery. LandTrendr characterizes temporal trajectories of (abrupt) change in timeseries of e.g. spectral indices and is suitable to detect location and date of mangrove ecosystem erosion and colonization. The coast of Suriname is selected because it is characterized by strong dynamics and still has pristine undisturbed stretches of mangrove forest. The dynamics of the Suriname coast are predominantly driven by migrating mudbanks, consisting of mud originating from the Amazon. The huge volumes of mud self-organize in banks and migrate from east to west and cause erosion or accretion at the coast in cycles of approximately 35 years (Augustinus, 1978; 1980, 2004; Augustinus et al., 1989; Anthony et al., 2008, 2010; World Bank, 2018). It is important to understand and quantify the response of mangrove ecosystems to these large-scale morphological changes, in order to elucidate the drivers behind natural temporal and spatial changes in mangrove colonization and erosion. Such knowledge is also needed to optimize coastal zone management. Especially in Suriname this is relevant because there is an ongoing discussion about the construction of flood barriers to protect the capital of Paramaribo and the low-lying coastal plains, or to stimulate mangrove ecosystems as natural coastal protection and to reduce economic activities close to the coast instead (World Bank, 2018). North of Paramaribo, at 'Weg naar Zee', an experimental Building with Nature mangrove project is ongoing under guidance of the University of Suriname. Acquisition of long-term information on spatial distribution of the mangrove vegetation communities is urgently needed to inform effective strategies for mangrove management, protection and restoration. As such, the research questions of this study are:

- What are the benefits and limitations of using timeseries of satellite images of Landsat to detect and follow mangrove cover changes?
- How robust is the quasi-automatic algorithm LandTrendr used here to detect mangrove dynamics?
- What are the most dynamic locations along the Suriname coast, currently and in the recent past?
- What is the impact of mud bank migration and resulting accretion and erosion on colonization of mangroves, over the last decades along the Suriname coast?

2. Study area

Suriname is located at the Guiana coastline bordered in the east by French-Guiana and in the west by Guiana (Fig. 1). The coast is low-lying and flat, making the Guianas vulnerable to impacts of sea level rise. The coast is characterized by tropical mangrove forest, which are undisturbed and pristine at various locations. Mangrove species dominating the swamps at the Guiana coasts are *Avicennia germinans* and *Laguncularia racemosa* on the mudflats, while *Rhizophora racemosa* and *Rhizophora mangle* are common in the estuarine swamp areas and along riverbanks where saline seawater is more diluted by constant freshwater input (Fromard et al. 2004; Proisy et al., 2009; Spalding et al., 2010). The coast is characterized by high dynamics caused by migrating mudbanks. The mud originates from the Amazon with an estimated average sediment yield of 1.2×10^9 ton/year (Anthony et al., 2010). These huge volumes of mud self-organize in banks and migrate from the Amazon to the Orinoco and cause erosion or accretion at the coast in cycles of approximately 35 years (Anthony et al., 2008, 2010, 2013, Augustinus, 1980, 2004; Augustinus et al., 1989; Brunier et al., 2019; Walcker et al., 2015; Anthony and Nicolas, 2012). Fig. 2 shows the erosion and accretion rate along the entire Suriname coast since 1947 based on aerial photographs and satellite images as surveyed by Augustinus (in Wong and Augustinus, 2017). Fig. 3a and 3b shows some pictures of typical coastal erosion and accretion. Here, we intend to focus on new possibilities using Landsat image timeseries to quasi-automatically map losses and gains, and simultaneously capture colonization patterns of mangrove vegetation. The tropical climate of the Guianas knows seasonal variations in trade winds that influence the morphology and migration of the mudbanks, a process which is not fully understood (Augustinus, 2004). In the period February and March, i.e. the short dry season, the North-East trade winds (3 to 9 m/s) are dominant and strong. In the long dry period, August to October, lighter winds are coming from the North-East and are more variable with respect to direction and strength (Augustinus, 1978). The tide is semi-diurnal reaching up to 2.5 m during spring tide. Extensive descriptions of relevant geomorphological processes and their forcing mechanisms are presented by Toorman et al. (2018), Anthony et al. (2010), Augustinus et al. (1989) and Augustinus (1978).

3. Data and methods

3.1. Historic satellite data archive

Recent developments in earth observations provide archives of satellite images. Landsat is the longest running operational set of platforms collecting images of the earth surface. Landsat 4, 5, 7 and 8 had comparable sensors, the Thematic Mapper, Enhanced Thematic Mapper, Enhanced Thematic Mapper Plus and Operational Land Imager. In terms of spatial resolution and spectral setting these sensors are suited for change detection since the eighties. The Landsat images are made available in the Historic Satellite Data Archive (HSDA) within Google Earth Engine: GEE (Gorelick et al., 2017; van Deijns et al., 2020) at spatial resolution of 30 by 30 m. GEE (GEE, 2020) is a cloud-based

Fig. 1. The Suriname coast and location names used in this paper. The capital of Paramaribo is located in the centre-right.

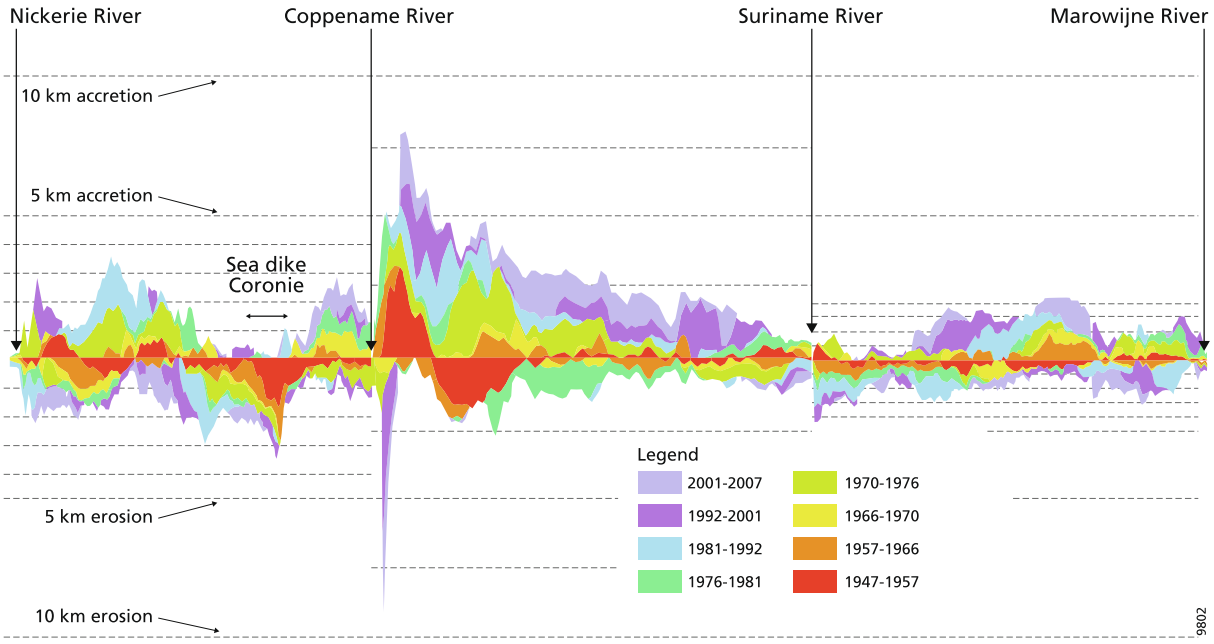

Fig. 2. Coastal erosion and accretion between 1947 and 2007 along the entire Suriname coast as surveyed by Augustinus (Wong et al., 2017).

geoprocessing platform providing a vast amount of publicly available geospatial datasets, including Landsat imagery, and facilitates fast data access and parallel processing for fast analysis capabilities (Gorelick et al., 2017; Kennedy et al., 2018). GEE data sets and scripts are used here for change analysis. Annual image availability for Suriname is nowadays around five to ten images with a revisit time of 16 days. A long time series would be an advantage as the full cycle of mud bank migration covers approximately 35 years. However, image quality and image availability before 2000 is low and for the year 1995 not one image of the study area is available in the archive. Therefore, we focus on the time period 2000 to 2018. The analysis method can easily be extended when more images are coming available in the archive.

3.2. *LandTrendr change algorithm*

To detect changes of mangrove coverage by coastal erosion or accretion and to detect the approximate rate and timing of these changes, the LandTrendr algorithm was applied to timeseries of satellite images. LandTrendr ('Landsat-based detection of trends in disturbance and recovery') provides a spectral-temporal segmentation algorithm useful for change detection in a time series of moderate resolution satellite imagery on a pixel-by-pixel basis while reducing background noise (Kennedy and Braaten, 2020; Kennedy et al., 2018). LandTrendr was originally developed for monitoring terrestrial forest disturbance and is suitable for detecting annual changes in vegetation cover induced by sudden events (Kennedy et al., 2012; Sengupta et al., 2019; van Deijns et al., 2020; Senf and Seidl, 2020; Hislop et al., 2020). LandTrendr is capable of analysing temporal trajectories of individual spectral bands and spectral indices. Here, we used Normalized Difference Vegetation Index (NDVI) values as input for LandTrendr, as NDVI values show useful and important contrasts between the green mangrove vegetation and grey-dark mudflats. Spectral vegetation indices like NDVI are particularly insightful in this context as mangrove vegetation is evergreen, and erosion and colonization can thus be detected year around. The Landsat images used here are all converted to surface reflectance (GEE User Guide, 2020). Due to cloud cover and shade it proved necessary to make a selection of satellite images acquired using functions for clouds and cloud-shadows (CF-masking functions).

The multi-dimensional median (medoid) technique is used to produce the best available yearly pixel composite. This Medoid method chooses the pixel value with minimum sum of squared differences between the median values and observations across bands. This composite method is robust against extreme pixel values and preserves the relationships between bands, because the pixel value selected is one of the observations of that pixel (Flood, 2013). With the best available pixel composite, LandTrendr uses a statistical fitting algorithm to segment spectral trajectories (Fig. 4). The algorithm is able to detect within continuous signals, i.e. in our case the NDVI-series, abrupt changes, gradual trends and time to recovery (Supplementary Information S1). It can separate long-duration signals from short-term noise originating from changes in sun angle, phenology and atmosphere conditions (Kennedy et al., 2012; Kennedy et al., 2010). This short-term noise is furthermore reduced by the medoid aggregation. The algorithm comprises several steps (Kennedy and Braaten, 2020; Kennedy et al., 2018)

Fig. 3a. Example of coastal erosion and mangrove loss near Kourou in French Guyana *(Photo. Steven M. de Jong, June 2019).*

Fig. 3b. Example of renewed accretion after coastal erosion at Weg naar Zee in Suriname *(Photo: Steven M. de Jong, June 2019).*

as shown in Fig. S1: removing spikes in the signal, identifying potential breakpoints by regression (Fig. S1b), culling segmentation by removing too small and local segments in (Fig. S1c) by angle change, fitting segments, streamlining segmentation by removing the weakest breakpoints (Fig. S1e), and selecting the best segmentation model using fitting statistics. Table S1 in the Supplementary data presents the eight LandTrendr parameter definitions. The outcome of the algorithm is, in our case, and determined after LandTrendr parameter evaluation, various maps for the entire Suriname coast of gain and loss of NDVI, or combinations of loss and gain, where NDVI is an indicator for erosion or settlement of mangrove ecosystems, and associated timing of the events.

To evaluate the robustness of the algorithms for mangrove change mapping, several parameter settings were run as scenarios to compare with the baseline (Table S2), and their segmentation results were compared at specific locations in the images. The standard settings are generally optimized, as indicated in the user manual, to detect abrupt changes in timeseries (Kennedy and Braaten, 2020). Based on an initial sensitivity analysis, three LandTrendr fitting parameters were selected for a more detailed evaluation (Table 1; S1): Maximum Segment (MS) is important for identification of breakpoints in the NDVI series. Recovery Threshold (RT) is used to filter out short-duration time segments shorter than a user-defined threshold. Best Model Proportion (BMP) controls the fitting of the trajectory and overfitting which might yield erroneous starts of the NDVI change event. Each parameter value was varied according to the values shown in Table 1 and the outcome was evaluated for 3000 reference points equally sampled over areas with loss, gain and loss & gain of NDVI values respectively.

3.3. Quantitative assessment of mangrove erosion and accretion

The timeseries of satellite images available allows monitoring locations of coastal dynamics, dating of erosive and accretion events and a quantitative assessment of surface areas of mangrove erosion and expansion. To quantify the surface area of mangrove recovery after erosion and colonization after retreat, we assessed the pixels where first erosion followed by accretion occurred in the time span 2000 to 2018 along the entire Suriname coast. By multiplying the number of identified pixels by the pixel size (30 by 30 m), we obtained annual surface areas of accretion and erosion. Next, it is of interest to compare our results with the results of Augustinus (in: Wong et al., 2017) shown in Fig. 2 because his overview dates back to 1947. Augustinus investigated the behaviour of the Suriname coastline in time and space by dividing the coastline into 339 sections, each with a width of 1 km. Net erosion/accumulation of the coast was measured by comparison of the various coastlines deduced from the available series of air photographs (1947/1948, 1957–1966–1970, 1981) and Landsat MSS and TM satellite images (1984–2007). The conversion of this linear displacement of the coast into tons per year has been achieved by multiplying the area of displacement in landward (−) or in seaward (+) direction for every km section, by the distance of displacement times the tangent of the nearshore slope (till the 3 m depth contour), and subsequently with the specific density of fresh clay (1850 kg of dry sediment per m3 of bulk wet sediment). A generalised slope angle of 0.6 degree has been used. The length of the mudbanks is determined in alongshore direction in the upper intertidal part of the banks. Although the timeseries has various gaps and the overview stops in 2007, the comparison and fusion enables the identification of long-term dynamic hot spots at the coast, detection of shifting patterns along the coast and evaluation of long-term area changes of erosion and accretion. Such comparison is not straightforward as Augustinus presents erosion and accretion along profiles in meters, approximately perpendicular on the coast, while our results yield square kilometres of erosion and accretion computed from the imagery and mainly based on mangrove presence. It should be noted, that although a basic coastal delineation was applied, some inland areas of NDVI change were detected as will be discussed in the discussion section.

3.4. Patterns of mangrove colonization

Fromard et al. (2004) present a detailed study on how mud bank dynamics at the French Guiana coast have an impact on the structure, composition and colonization patterns of the mangroves. This study used SPOT-XS images of 20 m resolution (1991, 1993, 1997, 1999) and aerial photographs (1951, 1955, 1966, 1999) covering a period of approximately 50 years, field studies and experiments. Visual interpretation of the images and photos yielded information on two mangrove types, mangrove area evolution i.e. erosion and accretion, and information on mangrove colonization processes and patterns. Three distinct colonization patterns were identified in their study (Fig. 5): (1) mangrove bands parallel to the coastline, which establish a regular zonation of the mangroves; (2) mangrove patch expansion where

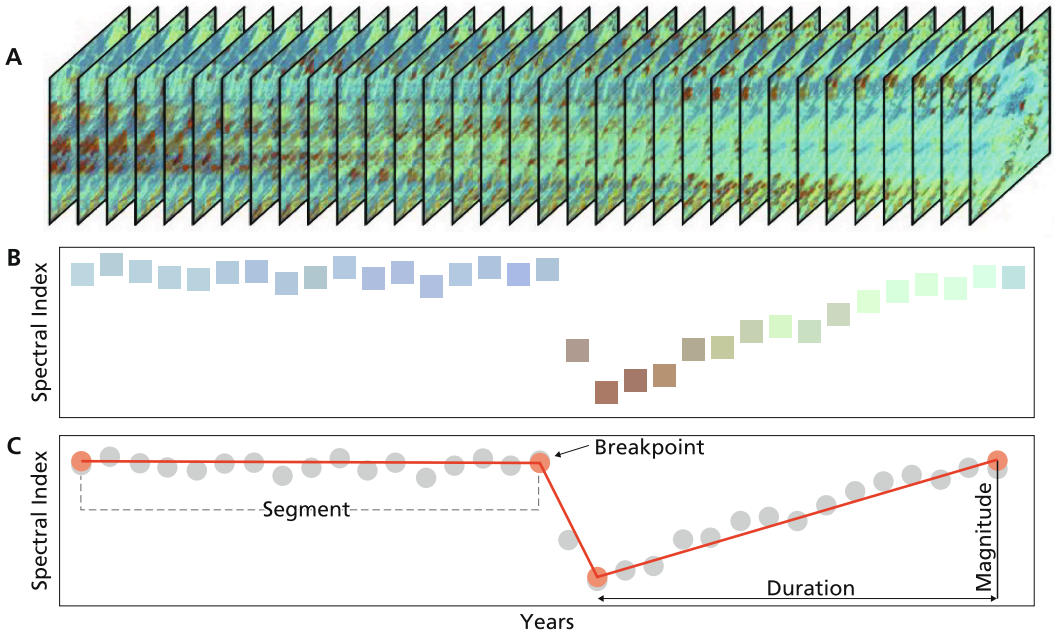

Fig. 4. Concept of the change detection algorithm of LandTrendr. Each pixel in the best available yearly composite between 2000 and 2018 (a), contributes to a trajectory of a spectral index i.e. NDVI (b). LandTrendr then detects magnitude, duration and timing of disturbance in the trajectory (c). Source: Kennedy and Braaten, 2020; Kennedy et al., 2018.

Table 1
The variations of LandTrendr control parameters next to standard settings evaluated here (Kennedy et al., 2010). Table S2 presents all the LandTrendr parameters used for best fitting to detect abrupt and gradual changes.

Parameters	Values
Max Segments	4
	6
	12
Recovery Threshold	0.25
	0.5
	0.75
Best Model Proportion	0.5
	1
	1.25

pioneer mangrove plants develop from residual mud patches that escaped erosion; and (3) arc-shaped patterns of colonization linked to the east–west directed mud bank and sediment migration, which leads to the formation of sedimentary bars, which are rapidly colonized by the pioneering mangrove. The relation between mudbanks and mangrove erosion or settlement is extremely difficult to determine because identifying mudbank location and migration speeds is extremely difficult (De Vries et al., 2021). In our study, we investigated whether the results and the spatial resolution of the quasi-automated Landtrendr method was capable of detecting similar colonization patterns. As such, spatial trends in colonization were visually analysed based on the gain and loss NDVI images resulting from the LandTrendr algorithm described in the previous section. The active periods of mangrove gain of the locations near Totness, Coppename and Wia-Wia were selected for this evaluation of patterns.

4. Results & discussion

The results of the LandTrendr analysis of Landsat NDVI images acquired between 2000 and 2018 are indicative for the spatio-temporal patterns of mangrove erosion and colonization and are discussed first. Next, the evaluation of the parameter setting and the fitting-trajectories based on the scenarios are presented.

4.1. Locations of mangroves loss and gain

Figs. 6 and 7 show the overall changes, gain or loss, of the NDVI-values, which are indicative for the dynamics of the mangrove coverage along the entire Suriname coast. It is estimated that when an area on a dark-grey mudflat has ≥20% mangrove vegetation cover it is detectable by a change in NDVI values. Fig. 6 shows the increase of mangroves (gain of NDVI) and Fig. 7 shows the decrease of mangroves (loss of NDVI). Colours indicate the change between 2000 and 2018 in intervals of three to four years. Fig. 6a highlights key hotspots of accretion and mangrove settlement. These hotspots are located east of the town of Totness (Fig. 6b) with increasing mangrove presence from 2004 to 2008 in the western part and from 2008 to 2011 in the eastern part. Other mangrove development areas are at Coppename Nature Reserve (Fig. 6c) mostly during the entire time span from 2004 until 2018, and near Wia-Wia Nature Reserve (Fig. 6d) starting in the east from 2000 and continuing westwards until 2014. Polygon clipping of the coastal area was applied because the emphasis of this study is on coastal mangroves, although this introduces some uncertainties and includes some other vegetation types than mangroves, such as inland swamps (see Fig. 6d).

Fig. 7 shows the hotspots of coastal erosion and mangrove loss. Important areas of loss of mangroves and land are at the coastal stretches west and east of the town of Nieuw Nickerie and at the outlet of the Corantijn River (Fig. 7a). From 2000 to 2018, erosion of mangroves is seen continuously. A short stretch of the coast of approximately 5 km is currently protected by a sea dike northwest of the town of Nieuw Nickerie and has stopped the erosion process at the outlet of the river (Fig. 7b).

A second important area of coastal erosion and mangrove loss is located west of Totness close to Hertenrits (Fig. 7c) showing an ongoing loss from 2000 and developing westwards to 2018 while a gain of mangroves develops to the east from 2011 onwards. This location illustrates the spatial shifts of erosion and accretion patterns and coastal

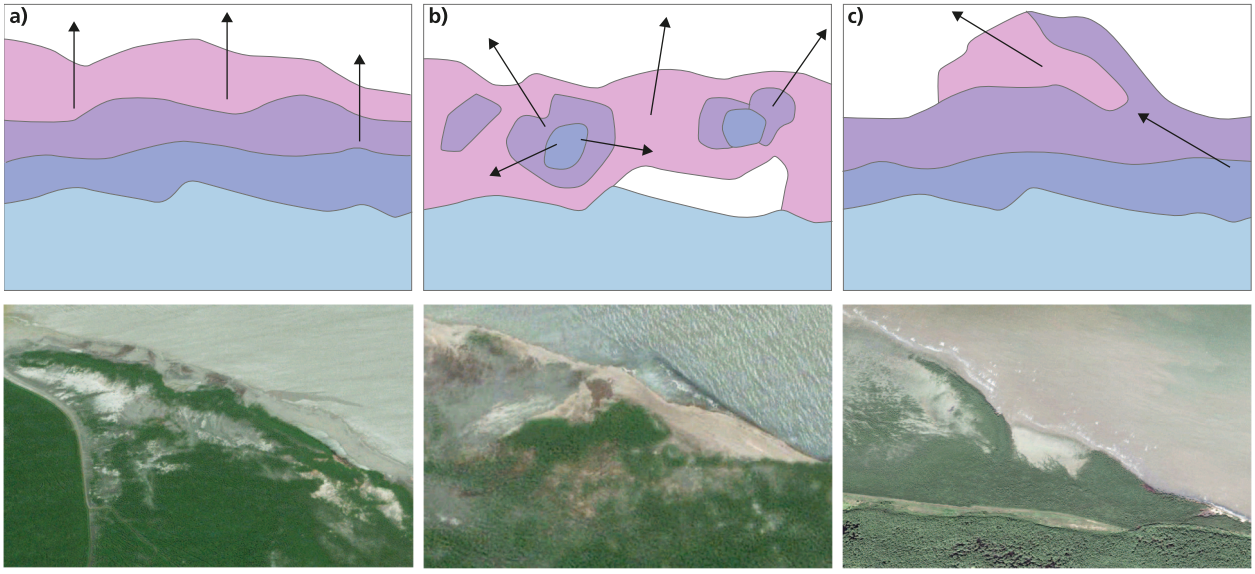

Fig. 5. Above: schematic sketch of patterns of mangrove colonization in the Sinnamary study area in French Guyana; (a) regular zonation, (b) patches and (c) arc-shaped (adapted from Fromard et al., 2004). Below: examples of RGB satellite images of Google maps showing similar patterns at the Suriname coast east of Matapica channel. The lower left image shows from west to east a green regular zone, band-shaped, of mangrove. The lower central image shows in its centre two connected patches. The lower right image shows an arc-shape mangrove belt in the left part. Note that the sand deposit in the lower centre example may have played a role in the patch formation. (For interpretation of the references to colour in this figure legend, the reader is referred to the web version of this article.)

processes and the added value of long timeseries of satellite imagery. Fig. 7d and e pinpoint to coastal erosion sites northwest of Paramaribo locally known as 'Weg naar Zee'. Coastal erosion is substantial here, causing damage to agricultural land and infrastructure and continues up to 2018. Therefore, the Anton de Kom University has initiated a 'Building with Nature' project, co-funded by Conservation International, on this location to stimulate mangrove restoration and development. Fig. 7f shows a small dynamic area of erosion at the east side of the coast of Suriname close to the Wia-Wia Nature Preserve.

4.2. Quantitative assessment of mangrove loss and gain

Our results provide quantitative analysis of year-by-year variations of mangrove dynamics. Fig. 8 shows the annual mangrove loss and gain during 2000 to 2018 only for the areas considered. Surface areas eroded, in red, range from 0.5 km^2 in 2002 and 2006 to almost 12 km^2 in 2015. Accretion, in green, shows the same dynamic pattern and gained area goes up to 11 km^2. A division is made between events where first mangrove loss and next gain was spotted in the imagery and vice versa to study the cyclic behaviour. In the mangrove recovery regions (Fig. 8b), the loss events mainly occurred before 2005, and the recolonization areas gradually increased and reached a maximum in 2010. In the mangrove loss after gain areas (Fig. 8a) the major colonization events occurred in 2007, and the eroding areas expanded until reaching a maximum in 2015.

The LandTrendr analysis also provides information on the duration of mangrove erosion before recolonization occurred and the duration of colonization before a shift to mangrove loss. These dynamics are driven by sediment depositions, mud bank dynamics and active current control by mangroves (Furukawa and Wolanski, 1996). Fig. 9 shows the relative areas as a percentage of total annual mangrove gain and loss, as a function of duration length between the gain and loss event at locations where colonization was followed by erosion, and erosion followed by colonization. For large areas, the settled and developed mangroves can be eroded after one to four years (Fig. 9a), whereas eroded mangroves can recover after five to nine years and faster in occasional cases (Fig. 9b). The timeseries available for this study is however too short to cover a full mud bank cycle which is approximately 30 years or longer. Short term colonization of mangroves of less than two years will also not be detected by LandTrendr as no temporal segments with breakpoints can be detected in such case. It should be noted that although a coastal delineation was applied, some inland changes of NDVI change were detected. These surface areas are however small and their effect on the estimated surface change is minimal. Still, results should be interpreted with care. The high recovery peak after one year in Fig. 9 seems unrealistically fast and further research is needed to understand the increases in NDVI values that cause the detection of this fast recolonization.

Comparison of our results with the results of Augustinus shown in Fig. 2 is not straightforward, as the overlap in time between the two analyses is limited and as discussed in the method section the approach of assessing erosion and accretion is different. Comparing Figs. 2, 6 and 7 it becomes apparent that in the overlapping period from 2000 to 2007, the same locations, prone to coastal erosion are identified, specifically Totness, Nieuw Nickerie, Weg-naar-Zee and Wia-Wia which show coastal retreats in both datasets. Comparing Figs. 2 and 8, the period 2001 to 2006 appears to be an active erosion period. The accretion rates for some locations, e.g. the point of Coppename, estimated by Augustinus are around 2 to 5 km over 50 years (on average 40 to 100 m/yr), except for some extremes. Our results in Fig. 7b to d show a similar order of magnitude. Erosion rates estimated by Augustinus are round 2 to 3 km for 50 years (on average 40 to 60 m/yr). The results shown in Fig. 7b, c and f show again similar magnitudes. The areas shown in Fig. 7d and e correspond less well but no explanation was found so far.

4.3. Patterns of mangrove settlement

The three patterns of mangrove settlement and expansion described by Fromard et al. (2004) were identified at various locations along the coast even using this somewhat course resolution of 30 by 30 m of Landsat. Fig. 6b shows the zonation expansion of mangroves (NDVI) along the coast, Fig. 6c displays the arc-shaped expansion of mangroves following the development of the mud banks and Fig. 6d shows a mixture of both: zonation and arcs. Patch development and initial settlement of mangroves are more difficult to detect and distinguish because these processes mainly occur at finer scales. The circles in Fig. 6b indicate patterns of zonal expansion of mangroves, the triangles in Fig. 6c represent arc-shaped expansion patterns of mangroves and the squares in Fig. 6d mark patch-shaped mangrove expansion. For the

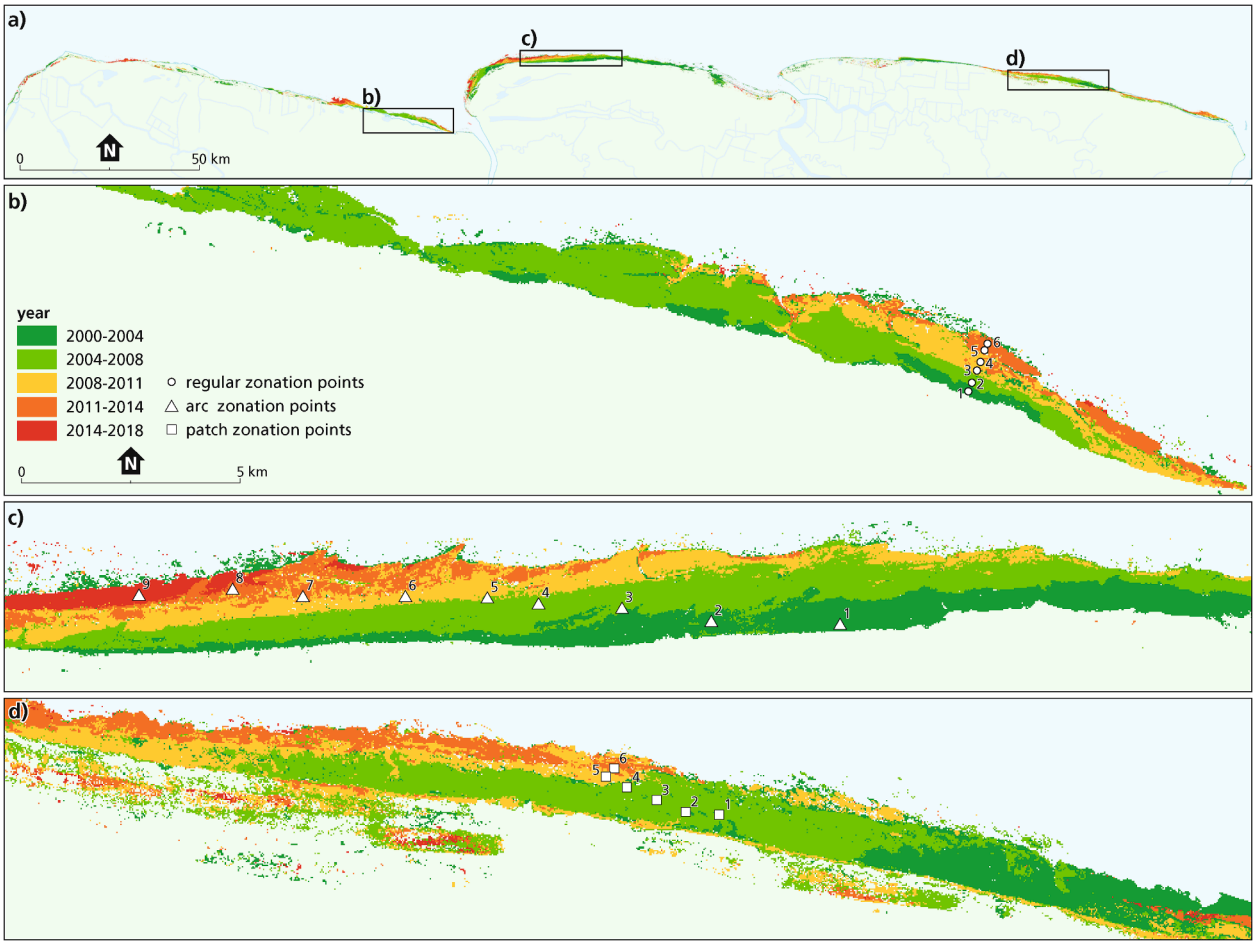

Fig. 6. Detected year of gain in NDVI values, corresponding to mangrove increase, which exceed the gain detection threshold derived from the baseline parameter set. Lightblue is the ocean, light green is land (Fig. 1 shows an overview of the study area). (a) An overview map and (b)–(d) detailed maps of Totness, Coppename and Wia-Wia respectively. Partial polygon clipping of the coastal region was applied which might introduce uncertaines in the mangrove areas due to inclusion of inland swamps in the classification. The regular zonation (circles), arc (triangles) and patch (squares) patterns of mangrove colonization as described by Fromard et al. (2004) are visible. Fig. 6b shows the zonation expansion of mangroves along the coast, Fig. 6c displays the arc-shaped expansion of mangroves following the development of the mud banks and Fig. 6d shows a mixture of both: zonation and arcs (further discussed in Section 4.3). (For interpretation of the references to colour in this figure legend, the reader is referred to the web version of this article.)

indicated locations, the NDVI development over time was analysed. NDVI values increased from around 0 until 0.7 within three years' time. When we assume that the NDVI increase on these mudflats is indicative for mangrove settlement and growth, it means that mangrove can colonize and develop within three years when the conditions are favourable. These findings match the observations of Fromard et al. (2004) describing colonization of mud banks by young mangroves within months to two years.

4.4. LandTrendr algorithm evaluation

The robustness of the LandTrendr algorithm to survey coastal dynamics was evaluated by running three scenarios for the three most important parameters settings i.e. Max Segments, Recovery Threshold and Best Model Proportion as shown in Table 1. Table 2 shows the summarizing statistics of this evaluation for the 3000 points sampled equally over areas with gain, areas with loss and combined loss and gain of NDVI values. The correlation refers to the observed and fitted trend for 1000 points for each of these tree areas (gains, losses, combined). The results of the baseline scenario are also presented in Table 2 and relate to the standard settings for LandTrendr (as detailed in Table S2). For the evaluation runs only one parameter setting was changed, and these were then compared to the results of the baseline settings. The scenario runs show differences in the identification of breakpoints, differences in the identified temporal segment length and recovery time and variations in the goodness of fits through the datapoints i.e. image acquisition dates. As an example, a high value of maximum allowable segments is required to identify all mangrove change events, but too many allowable segments increases the chances of false positives i.e. identification of segments and breakpoints but no mangrove change event. Best correlations are indicated in bold.

The baseline settings show a good performance in detecting the breakpoints in the timeseries and therefore in detecting erosion or accretion of mangrove areas. At locations where there is a combined loss and gain of NDVI values within the time span of 18 years, increasing the number of maximum segments has a modest positive effect on the correlation (Fig. S2). The effect of decreasing the values of the Recovery Threshold from 0.5 to 0.25 has a deteriorating effect as mangrove areas that are visually identified as recovering are excluded, leading to wrong identification of recovery timing (Fig. S3). A decrease of the Best Model Proportion to 0.5 yields better results and enhances the ability to capture the timing of change events, although the result might show overfitting at some locations, resulting in false identification of small change events (Fig. S4).

The correlation only becomes much lower when the best model proportion is set to 1.25, other changes of the correlation are small

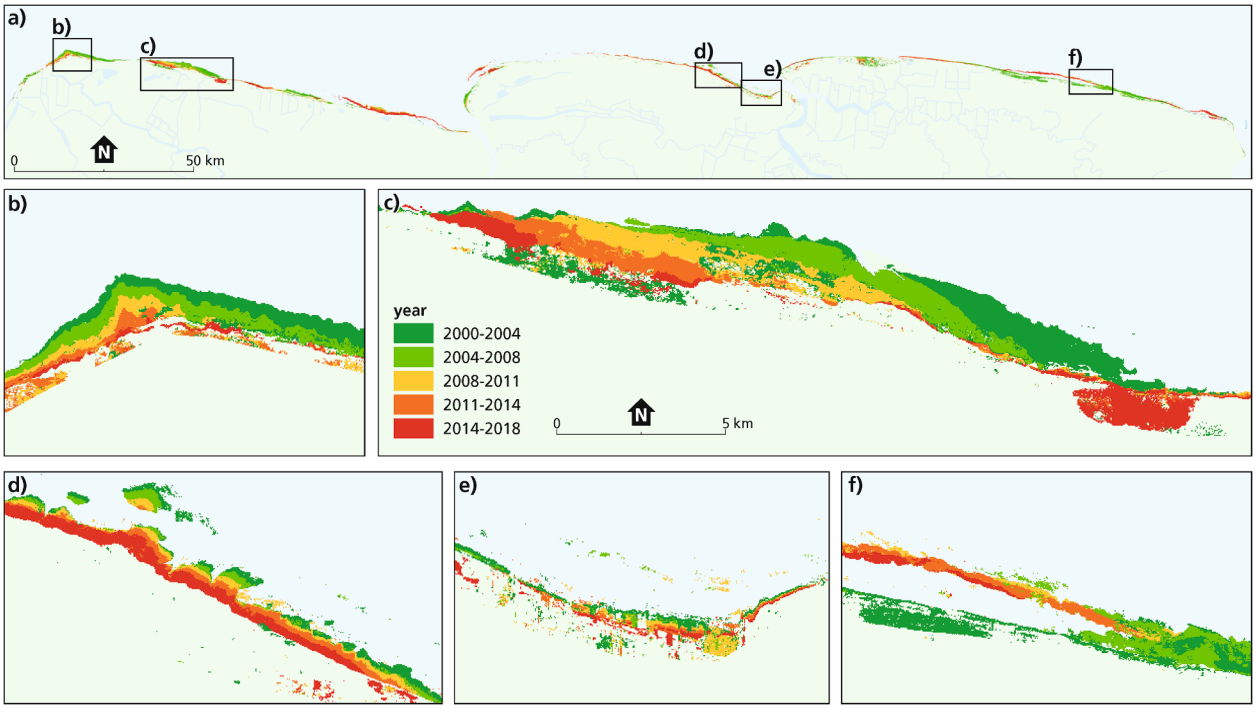

Fig. 7. Detected year of loss in NDVI values, indicating decrease of mangrove coverage, which exceed the LandTrendr loss detection threshold derived from the baseline parameter set. Partial polygon clipping of the coastal region was applied which might introduce uncertaines in the mangrove areas due to inclusion of inland swamps in the classification. An overview map of selected locations (a) and detailed maps of Nieuw Nickerie (b), Totness (c), Weg-naar-Zee west (d), Weg-naar-Zee (e) and Wia-Wia (f) (e) respectively.

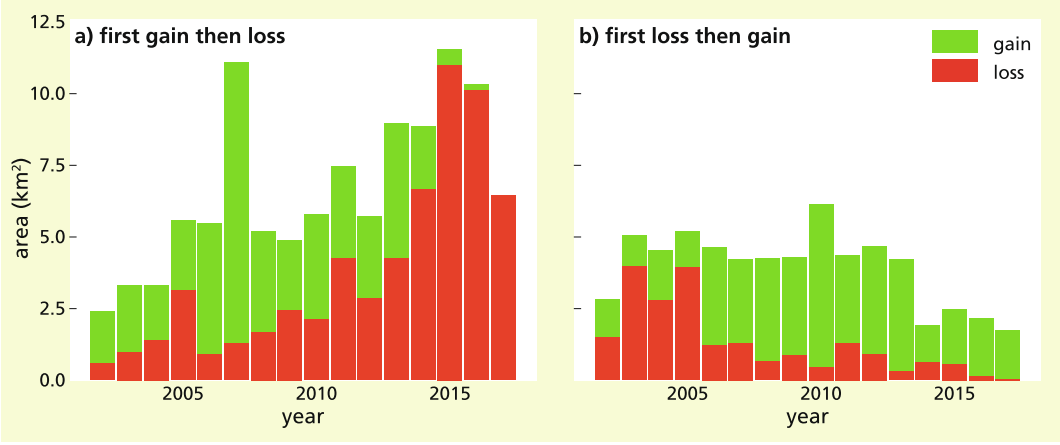

Fig. 8. Total area of annual mangrove gain and loss between 2000 and 2018 for the considered loss and gain areas separated in events where (a) colonization was followed by erosion, and where (b) erosion was followed by colonization.

indicating that the approach is rather robust. It should be noted that these LandTrendr settings were only evaluated for our study areas. When applying this method to other mangrove areas in the world, the parameter settings will therefore need careful consideration and testing.

4.5. *Mangrove surveying from satellite imagery timeseries*

The availability of satellite image archives has recently triggered many studies on mangrove dynamics derived from remote sensing. This includes studies focussing on coastal areas where mangroves have expanded or recovered, similar as here. Otero et al. (2020), for example, also used Landsat annual timeseries to assess recovery times of clear-felling or disturbance of mangrove ecosystems in Malaysia. They found mangrove recovery times ranging from 3 to 8 years. These results match our observations for the Suriname coast although mangroves for some of our sites recover over shorter time periods and within 3 years given favourable circumstances. Another mangrove system that has been investigated in detail through remote sensing is that of the Mekong delta in Vietnam. Nardin et al. (2016) focussed on the spatial and temporal mangrove canopy evolution using timeseries of Landsat imagery and Shuttle Radar Topography Mission (SRTM) elevation data, also using NDVI timeseries. They yielded linear-shaped and patched-shaped zones and speeds of mangrove canopy expansion which could be linked to less or more favourable conditions (related to wave exposure, and erosion and deposition patterns) for mangrove seedlings establishment. Their results somewhat resemble the three patterns of patch, regular zone and arc-shaped colonization we were able to identify at the Suriname coast, although the latter is perhaps more exclusive to coastal

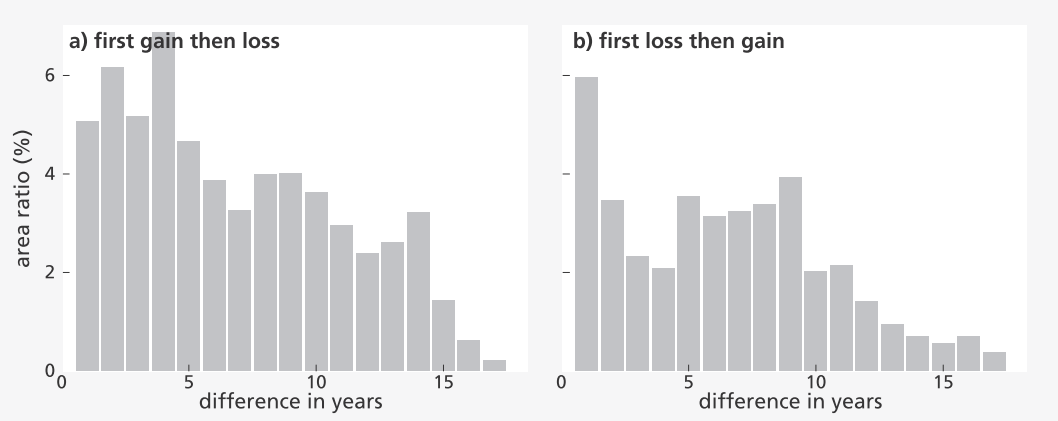

Fig. 9. Relative areas in percentage of annual mangrove gain and loss events between 2000 and 2018 as a function of the duration length between colonization and erosion events, either where (a) mangrove gain happened first or (b) mangrove loss happened first. The graph illustrates shifting and some cyclic behaviours of erosion and accretion but longer timeseries are needed to grasp an entire mudbank migration cycle.

Table 2
Statistics of the three evaluations of the robustness of the LandTrendr algorithm. The correlation refers to the observed and fitted trend for 1000 points for each of these three areas (loss, gain, combination of loss & gain). Best correlations are given in bold. Table S2 shows default LandTrendr values and other not here evaluated parameters.

		Combination (1000x)		only Loss (1000x)		only Gain (1000x)	
		Total no of breakpoints	Correlation	Total no of breakpoints	Correlation	Total no of breakpoints	Correlation
Baseline		4767	0.972	3889	0.978	3993	**0.986**
Max Segments	4	3786	0.923	3550	0.970	3732	0.979
	6	4542	0.962	3805	0.976	3921	0.984
	12	4772	**0.973**	3892	0.978	4012	0.986
Recovery Threshold	0.25	3822	0.930	3755	0.976	2862	0.940
	0.5	4454	0.960	3845	0.978	3763	0.979
	0.75	4736	0.970	3877	0.978	3987	0.984
Best Model Proportion	0.5	4830	**0.973**	3944	**0.979**	4036	**0.986**
	1	4690	0.970	3825	0.978	3942	0.985
	1.25	2000	0.546	2000	0.597	2000	0.523

systems with complex alongshore-directed mud transport as in the Guianas. Bullock (2017) then dived further into the study of the Mekong mangroves, using Landsat timeseries to map various development stages. They used Tasselled Cap transformed images, providing information on brightness, greenness and wetness, to distinguish distinct stages of forest development and detect turnover of mangrove species. They encountered similar problems as we did in our study, arising from limited satellite image availability because of cloud cover, sensor failure and changing image acquisition strategies. Their approach of using Tasselled Cap transformed variables, instead of the NDVI spectral index applied here in the LandTrendr algorithm, is interesting and deserves further study to test whether it can also benefit the analysis of mangrove behaviour at the Surinam coast. The NDVI has been criticized because of atmospheric impact, saturation effects and and sensor issues (Huang, 2020), future studies may evaluate whether the Tasselled Cap approach or indices such as the Modular Mangrove Recognition Index (MMRI) proposed by Diniz et al. (2019) using a combined ratio of the NDVI and the NDWI (Normalized Difference Water Index) yields better results in identifying mangroves on tidal flats and cover changes. Closer to our study site, focussing on mangrove dynamics in neighbouring French-Guiana, Walcker et al. (2015) reports about a comprehensive study to unravel the relation between mangrove extent and large scale atmospheric drivers over decadal timescales. They found that mangrove forest changes are linked to the multi-decadal fluctuations in trade wind-generated waves associated with the North Atlantic Oscillation (NAO). In addition to migrating mudbanks, these NAO variations, trade wind variations, and varying wave fronts may play a role in the complex mangrove and mud dynamics along the local coasts.

Over recent years, clearly much progress has been made in studying mangrove coasts by utilizing the growing availability of satellite imagery through a range of different techniques. LandTrendr has previously proven to be effective in detecting change in a range of different environments, but its applicability in dynamic mangrove environments has so far been limited. To our knowledge, this is the first study that uses LandTrendr to detect both mangrove colonization, erosion and combinations of both. We show that LandTrendr provides a robust and semi-automated approach that proves to be effective in detecting mangrove dynamics over large spatial and temporal scales. The resemblance in the order of magnitude between Augustinus' visual surveying of accretion and erosion and our semi-automatic LandTrendr approach provides confidence in the long-term trends, in the LandTrendr algorithm and its usefulness to analyse historic and newly available satellite images. The LandTrendr approach provides more informative quantitative information in terms eroded or deposited areas, expressed in square kilometres. A possible way to improve the LandTrendr results in this application might be to apply land masks to separate swamps and agricultural areas from mangroves in the images. As is visible in Figs. 6 and 7, mangroves are detected by the algorithm far land inward and this may be erroneous. We decided not to apply a land mask as tidal areas are large and not very well defined; applying a land mask could therefore result in neglecting mangrove areas. As such, further field surveys and validation field datasets are required for detailed land cover mapping. It is also important to note that with our analyses changes in mangrove presence can be detected but causes for these changes i.e. natural erosion, human disturbance, natural colonization or stimulated colonization cannot be determined.

5. Conclusions

Mangroves are important ecosystems in tropical areas for a range of ecosystem services including coastal protection, provision of habitats for fauna and flora (biodiversity), nursery function for fishes and crustaceans, and carbon sequestration. Relatively intact mangrove forests are still widely present along the coast of Suriname but they are under pressure. The Landsat satellite image archive, in combination with the LandTrendr algorithm, proved useful to study the dynamics of mangrove forest along this highly dynamic coast. As the archive is growing back in time as more historic images are added, and growing into the future, the timespan that we can study this coast will grow leading to an improved understanding. The annual composite images enable detecting the timing of coastal change and mangrove occupation. Changes in NDVI-values are assumed to be representative for the dynamics of mangroves on the mudflats in front of the Suriname coast, indicating erosion or expansion of mangrove vegetation. Some confusion with other vegetation, swamps and agriculture field, cannot be excluded in spite polygon clipping of coastal areas. Quantitative estimates of gain or loss in mangrove coverage is straightforward from the LandTrendr outputs. Change in mangrove surface area, considering the entire Suriname coast, can reach up to 12 km^2 for some years. Comparison with the visual interpretations by Augustinus provides confidence in the results derived from LandTrendr. Results were further validated by visual inspection of 3000 transects located at mangrove erosion sites, mangrove colonization sites and combinations of both between 2000 and 2018. Areas dominated by mangrove erosion were identified and are located near Copename, Nieuw Nickerie, Wia-Wia and Weg naar Zee. Spatial patterns of mangrove colonization and growth, in terms of the zonal-, arc- or patch-shaped patterns, were also identified at various locations, although the spatial resolution of Landsat may not allow for identification of all patterns present. For some locations, the occupation of the mudflats by mangroves, and corresponding increases of NDVI-values from ~0 to ~0.7 occurred within three years, indicating high colonization speeds. Information on these recovery speed is important for rehabilitation efforts and Building with Nature projects. Parameter setting in LandTrendr is important and key for successful mapping of mangrove dynamics. The number of maximum segments and best model proportion appear to be important parameters for identifying the correct timing of dynamic changes in mangrove, while the recovery threshold is essential for capturing recovery events. Overall, LandTrendr provides a robust and semi-automated approach to study mangrove dynamics over larger spatial and temporal scales. The relation between mangrove dynamics and mud bank position and migration speed is still not clear but longer time series analyses may be helpful to clarify this. Portability of the method to mangrove ecosystems elsewhere is feasible but requires careful attention regarding parameter settings. Combined studies to mangroves, mudbanks, ocean currents and trade winds are required to improve our understanding of the coastal ecosystem and to develop sustainable coastal protection methods with a role for mangroves.

CRediT authorship contribution statement

Steven M. de Jong: Supervision, Funding acquisition. **Youchen Shen:** Conceptualization, Methodology, Software. **Job de Vries:** Conceptualization, Methodology, Software. **Ginny Bijnaar:** Writing - review & editing. **Barend van Maanen:** Conceptualization, Writing - original draft, Supervision. **Pieter Augustinus:** Writing - review & editing. **Pita Verweij:** Supervision, Writing - review & editing, Funding acquisition.

Declaration of Competing Interest

The authors declare that they have no known competing financial interests or personal relationships that could have appeared to influence the work reported in this paper.

Acknowledgements

This project was financially supported by the NWO WOTRO Joint Sustainability Development Goal Research Program (Grant no. W07.303.106) and by the Utrecht University Bright Minds project.

Appendix A. Supplementary material

Supplementary data to this article can be found online at https://doi.org/10.1016/j.jag.2020.102293.

References

Alongi, D.M., 2002. Present state and future of the world's mangrove forests. Environ. Conserv. 29 (3), 331–349. https://doi.org/10.1017/S0376892902000231.

Anthony, E.J., Dolique, F., Gardel, A., Gratiot, N., Proisy, C., Polidori, L., 2008. Nearshore intertidal topography and topographic-forcing mechanisms of an Amazon-derived mud bank in French Guiana. Cont. Shelf Res. 28, 813–822. https://doi.org/10.1016/j.csr.2008.01.003.

Anthony, E.J., Gardel, A., Gratiot, N., Proisy, C., Allison, M.A.M.A., Dolique, F., Fromard, F.F., 2010. The Amazon-influenced muddy coast of South America: a review of mud-bank-shoreline interactions. Earth-Sci. Rev. 103, 99–121. https://doi.org/10.1016/j.earscirev.2010.09.008.

Anthony, E.J., Nicolas, Gratiot, 2012. Coastal engineering and large-scale mangrove destruction in Guyana, South America: averting an environmental catastrophe in the making. Ecol. Eng. 47, 268–273. https://doi.org/10.1016/j.ecoleng.2012.07.005.

Anthony, E.J., Gardel, A., Proisy, C., Fromard, F., Gensac, E., Peron, C., Walcker, R., Lesourd, S., 2013. The role of fluvial sediment supply and river-mouth hydrology in the dynamics of the muddy, Amazon-dominated Amapá-Guianas coast, South America: a three-point research agenda. J. South Am. Earth Sci. 44, 18–24. https://doi.org/10.1016/j.jsames.2012.06.005.

Augustinus, P.G.E.F., 1978. The changing shoreline of Suriname (South America). Published by "Natuurwetenschappelijke Studiekring voor Suriname en de Nederlandse Antillen", vol. 95. PhD Dissertation, Utrecht University. The Netherlands.

Augustinus, P.G.E.F., 1980. Actual development of the chenier coast of Suriname (South America). Sediment. Geol. 26, 91–113. https://doi.org/10.1016/0037-0738(80)90007-X.

Augustinus, P.G.E.F., 2004. The influence of the trade winds on the coastal development of the Guianas at various scale levels: a synthesis. Mar. Geol. 208, 145–151. https://doi.org/10.1016/j.margeo.2004.04.007.

Augustinus, P.G.E.F., Hazelhoff, L., Kroon, A., 1989. The chenier coast of Suriname: modern and geological development. Mar. Geol. 90, 269–281. https://doi.org/10.1016/0025-3227(89)90129-1.

Balke, Thorsten, Webb, E.L., Van den Elzen, E., Galli, D., Herman, P.M.J., Bouma, T.J., 2013. Seedling establishment in a dynamic sedimentary environment: a conceptual framework using mangroves. J. Appl. Ecol. 50, 740–747. https://doi.org/10.1111/1365-2664.12067.

Balke, T., Herman, P.M.J., Bouma, T.J., 2014. Critical transitions in disturbance-driven ecosystems: Identifying windows of opportunity for recovery. J. Ecol. 102 (3), 700–708. https://doi.org/10.1111/1365-2745.12241.

Barbier, E.B., Hacker, S.D., Kennedy, C., Koch, E.W., Stier, A.C., Silliman, B.R., 2011. The value of estuarine and coastal ecosystem services. Ecol. Monogr. 81, 169–193. https://doi.org/10.1890/10-1510.1.

Brunier, G., Anthony, E.J., Gratiot, N., Gardel, A., 2019. Exceptional rates and mechanisms of muddy shoreline retreat following mangrove removal. Earth Surf. Proc. Land. 44, 1559–1571. https://doi.org/10.1002/esp.4593.

Bullock, E.L., Fagherazzi, S., Nardin, W., Vo-Luong, P., Nguyen, P., Woodcock, C.E., 2017. Temporal patterns in species zonation in a mangrove forest in the Mekong Delta, Vietnam, using a time series of Landsat imagery. Continental Shelf Res. 147, 144–154. https://doi.org/10.1016/j.csr.2017.07.007.

Copernicus, 2020. European Space Agency (ESA) Data and Information Access Services (DIAS) https://www.copernicus.eu/en/access-data/dias.

van Deijns, A.A.J.F., Zadelhoff, A., Bevington, S.M De, Jong, M., Geertsema, S McDougall, 2020. Semi-automated detection and dating of landslides using harmonic modelling, Buckinghorse River, Canada. Int. J. Appl. Earth Observ. Geoinform. 84 https://doi.org/10.1016/j.jag.2019.101943.

De Vries, J., van Maanen, B., Ruessink, G., Verweij, P.A., de Jong, S.M., 2021. Unmixing water and mud: characterizing diffuse boundaries of subtidal mud banks from individual satellite observations. Int. J. Appl. Earth Observ. Geoinform. 95, 1–12. https://doi.org/10.1016/j.jag.2020.102252.

Diniz, C., Cortinhas, L., Nerino, G., Rodrigues, J., Sadeck, L., Adami, M., Souza-Filho, P. W.M., 2019. Brazilian mangrove status: three decades of satellite data analysis. Remote Sens. 11, 1–19. https://doi.org/10.3390/rs11070808.

Flood, N., 2013. Seasonal composite landsat TM/ETM+ images using the medoid (a multi-dimensional median). Remote Sens. 5, 6481–6500. https://doi.org/10.3390/rs5126481.

Fromard, F., Vega, C., Proisy, C., 2004. Half a century of dynamic coastal change affecting mangrove shorelines of French Guiana. A case study based on remote sensing data analyses and field surveys. Mar. Geol. 208, 265–280. https://doi.org/10.1016/j.margeo.2004.04.018.

Furukawa, K., Wolanski, E., 1996. Sedimentation in mangrove forests. Mangroves Salt Marshes 1, 3–10.
GEE, 2020. Google Earth Engine Time-lapse: a global zoomable video illustrating earth surface dynamics for images in the archive from ~1984 onwards. https://earthengine.google.com/timelapse/ Accessed on 22 December 2020.
User Guide, 2020. Google Earth Engine User Guide Landsat Algorithms. https://developers.google.com/earth-engine/guides/landsat. Accessed on 22 December 2020.
Gorelick, N., Hancher, M., Dixon, M., Ilyushchenko, S., Thau, D., Moore, R., 2017. Google Earth Engine: Planetary-scale geospatial analysis for everyone. Remote Sens. Environ. 202, 18–27. https://doi.org/10.1016/j.rse.2017.06.031.
Hamilton, S.E., Friess, D.A., 2018. Global carbon stocks and potential emissions due to mangrove deforestation from 2000 to 2012. Nat. Clim. Change 8 (3), 240–244.
Helder, D., Markham, B., Morfitt, R., Storey, J., Barsi, J., Gascon, F., Clerc, S., LaFrance, B., Masek, J., Roy, D., Lewis, A., 2018. Observations and recommendations for the calibration of Landsat 8 OLI and Sentinel 2 MSI for improved data interoperability. Remote Sens. 10 https://doi.org/10.3390/rs10091340.
Hislop, S., Haywood, A., Jones, S., Soto-Berelov, M., Skidmore, A., Nguyen, T.H., 2020. A satellite data driven approach to monitoring and reporting fire disturbance and recovery across boreal and temperate forests. Int. J. Appl. Earth Observ. Geoinform. 87, 102034, 1–14. https://doi.org/10.1016/j.jag.2019.102034.
Hu, Z., van Belzen, J., van der Wal, D., Balke, T., Wang, Z.B., Stive, M., Bouma, T.J., 2015. Windows of opportunity for salt marsh vegetation establishment on bare tidal flats: the importance of temporal and spatial variability in hydrodynamic forcing. J. Geophys. Res. Biogeosci. 120, 1450–1469. https://doi.org/10.1002/2014JG002870.
Huang, S., Tang, L., Hupy. J.P., Wang, Y., Shao, G., 2020. A commentary review on the use of normalized difference vegetation index (NDVI) in the era of popular remote sensing. J. Forest. Res. 31. https://doi-org.proxy.library.uu.nl/10.1007/s11676-020-01155-1.
Kennedy, R.E., Yang, Z., Cohen, W.B., 2010. Detecting trends in forest disturbance and recovery using yearly Landsat time series: 1. LandTrendr — Temporal segmentation algorithms. Remote Sens. Environ. 114 (12), 2897–2910. https://doi.org/10.1016/j.rse.2010.07.008.
Kennedy, R.E., Yang, Z., Cohen, W.B., Pfaff, E., Braaten, J., Nelson, P., 2012. Spatial and temporal patterns of forest disturbance and regrowth within the area of the Northwest Forest Plan. Remote Sens. Environ. 122, 117–133. https://doi.org/10.1016/j.rse.2011.09.024.
Kennedy, R.E., Yang, Z., Gorelick, N., Braaten, J., Cavalcante, L., Cohen, W., Healey, S., 2018. Implementation of the LandTrendr Algorithm on Google Earth Engine. Remote Sens. 10(5).10.3390/rs10050691.
Kennedy, R.E., Braaten, J., 2020. Guide to the Google Earth Engine implementation of the LandTrendr spectral-temporal segmentation algorithm. Available on line: https://emapr.github.io/LT-GEE/index.html Accessed on 1 October 2020.
Lewis, R.R., 2005. Ecological engineering for successful management and restoration of mangrove forests. Ecol. Eng. 24, 403–418. https://doi.org/10.1016/j.ecoleng.2004.10.003.
Liu, M., Zhang, H., Lin, G., Lin, H., Tang, D., 2018. Zonation and directional dynamics of mangrove forests derived from time-series satellite imagery in Mai Po, Hong Kong. Sustainability 10 (1913), 1–16. https://doi.org/10.3390/su10061913.
Liu, W.C., Hsu, M.-H., Wang, C.-F., 2003. Modeling of flow resistance in mangrove swamp at Mouth of Tidal Keelung River, Taiwan. J. Waterway Port Coastal Ocean Eng. 129 (2), 85–92. https://doi.org/10.1061/(ASCE)0733-950X(2003)129:2(86).
NASA-EO (Earth Observation), 2020. Cloud fraction maps 2000-2020. Accessed on 1 October 2020.
Nardin, W., Locatelli, S., Pasquarella, V., Rulli, M.C., Woodcock, C.E., Fagherazzi, S., 2016. Dynamics of a fringe mangrove forest detected by Landsat images in the Mekong River Delta, Vietnam. Earth Surf. Process. Landforms 41, 2024–2037. https://doi.org/10.1002/esp.3968.
Otero, V., Van De Kerchove, R., Satyanarayana, B., Mohd-Lokman, H., Lucas, R., Dahdouh-Guebas, F., 2020. An analysis of the early regeneration of mangrove forests using landsat time series in the Matang mangrove forest reserve, Peninsular Malaysia. Remote Sens. 11 (774), 1–18. https://doi.org/10.3390/rs11070774.
Proisy, C., Gratiot, N., Anthony, E.J., Gardel, A., Fromard, F., Heurete, P., 2009. Mud bank colonization by opportunistic mangroves: a case study from French Guiana using lidar data. Cont. Shelf Res. 29, 632–641. https://doi.org/10.1016/j.csr.2008.09.017.
Richards, D.R., Friess, D.A., 2016. Rates and drivers of mangrove deforestation in Southeast Asia, 2000–2012. Proc. Natl. Acad. Sci. 113 (2), 344–349.
Saintilan, N., Khan, N.S., Ashe, E., Kelleway, J.J., Rogers, K., Woodroffe, C.D., Horton, B. P., 2020. Thresholds of mangrove survival under rapid sea level rise. Science 368, 1118–1121. https://doi.org/10.1126/science.aba2656.
Senf, C., Seidl, R., 2020. Mapping the forest disturbance regimes of Europe. Nat. Sustain. 9, 1–17. https://doi.org/10.1038/s41893-020-00609-y.
Sengupta, D., Chen, R., Meadows, M.E., Choi, Y.R., Banerjee, A., Zilong, Xia, 2019. Mapping trajectories of coastal land reclamation in nine deltaic megacities using google earth engine. Remote Sens. 11 (2621), 1–13. https://doi.org/10.3390/rs11222621.
Spalding, M., Kainuma, M., Collins, L., 2010. World Atlas of Mangroves. Earthscan from Routledge. ISBN: 978-1-84407-657-4. 319p.
Toorman, E.A., Anthony, E., Augustinus, P.G.E.F., Gardel, A., Gratiot, N., Homenauth, O., Huybrechts, N., Monbaliu, J., Moseley, K., Naipal, S., 2018. Interaction of mangroves, coastal hydrodynamics, and morphodynamics along the coastal fringes of the Guianas. In: Makowski, C., Finkl, C.W. (eds.), Threats to Mangrove Forests, pp. 429–473. doi:10.1007/978-3-319-73016-5_20.
Van Bijsterveldt, C.E.J., van Wesenbeeck, B.K., van der Wal, D., Afiati, N., Pribadi, R., Brown, B., Bouma, T.J., 2020. How to restore mangroves for greenbelt creation along eroding coasts with abandoned aquaculture ponds. Estuar. Coast. Shelf Sci. 235 https://doi.org/10.1016/j.ecss.2019.106576.
Van Maanen, B., Coco, G., Bryan, K.R., 2015. On the ecogeomorphological feedbacks that control tidal channel network evolution in a sandy mangrove setting. Proc. R. Soc. A. 47120150115 10.1098/rspa.2015.0115.
Walcker, R., Anthony, E.J., Cassou, C., Aller, R.C., Gardel, A., Proisy, C., Martinez, J.-M., Fromard, F., 2015. Fluctuations in the extent of mangroves driven by multi-decadal changes in North Atlantic waves. J. Biogeogr. 42, 2209–2219. https://doi.org/10.1111/jbi.12580.
Winterwerp, J.C., Wilms, T., Siri, H.Y., van Thiel de Vries, J., Noor, Y.R., Van Wesenbeeck, B., Cronin, K., Van Eijk, P., Tonneijck, F., 2016. Building with nature: sustainable protection of mangrove coasts. Terra et Aqua 144, 5-12. Available at: https://www.iadc-dredging.com/.
Winterwerp, J.C., Erftemeijer, P.L.A., Suryadiputra, N., van Eijk, P., Zhang, Liquan, 2013. Defining eco-morphodynamic requirements for rehabilitating eroding mangrove-mud coasts. Wetlands 33, 515–526. https://doi.org/10.1007/s13157-013-0409-x. 912.
Wong, T.S., Kroonenberg, Augustinus, P., 2017. Geologie en landschap van Suriname. LM Publishers, Volendam (in Dutch). ISBN 978-94-6022-459-1.
World Bank, 2018. Suriname Coastal Resilience assessment. Technical Report 130439. Available online: https://www.researchgate.net/publication/331160395_Suriname_Coastal_Resilience_Assessment (Accessed on October 2020).
Xie, D., Schwarz, C., Bruckner, M.Z.M., Kleinhans, M.G., Urrego, D.H., Zhou, Z., van Maanen, B., 2020. Mangrove diversity loss under sea-level rise triggered by bio-morphodynamic feedbacks and anthropogenic pressures. Environ. Res. Lett. 15 https://doi.org/10.1088/1748-9326/abc122.
Yang, S.L., Li, H., Ysebaert, T.J., Bouma, T.J., Zhang, W.X., Li, P., Li, M., Ding, P.X., 2008. Spatial and temporal variations in 914 sediment grain size in tidal wetlands, yangtze delta: on the role of 915 physical and biotic controls. Estuarine, Coastal Shelf Sci. 916 77 (4), 657–671. https://doi.org/10.1016/j.ecss.2007.10.024.
Zhua, Z., Wulder, M.A., Roy, D.P., Woodcock, C.E., Hansen, M.C., Radeloff, V.C., Healey, S.P., Schaaf, C., Hostert, P., Strobl, P., Pekel, J.F., Lymburner, L., Pahlevan, N., Scambosm, T.A., 2019. Benefits of the free and open Landsat data policy. Remote Sens. Environ. 224, 382–385. https://doi.org/10.1016/j.rse.2019.02.016.